DOI 10.5162/Ultrasonic2025/A18-a1

Modeling and simulation of the behavior of piezoceramics with the discontinuous Galerkin method

Carsten Spieker[1], Jonas Hölscher[2], Leander Claes[2], Bernd Henning[2], and Jens Förstner[1]
[1] Theoretical Electrical Engineering Group, Paderborn University, 33098 Paderborn, Germany
[2] Measurement Engineering Group, Paderborn University, 33098 Paderborn, Germany
carsten.spieker@uni-paderborn.de

Abstract: This paper explores the use of the discontinuous Galerkin time domain method (DG) for simulating piezoceramics, which is essential in designing ultrasonic transducers. The DG method allows computational efficiency and provides good adaptability to three-dimensional structures. The study confirms the method's stability and accuracy, emphasizing the importance of proper boundary conditions and computational grids, which set the stage for future developments.

Keywords: Discontinuous Galerkin Time Domain Method, Piezoelectricity, Material characterization, Numerical flux, Parallelization

Motivation

Physics-based numerical simulations of piezoceramics are essential for the design of components such as ultrasonic transducers. In this work, we investigate the application of the discontinuous Galerkin time domain method (DG) to solve a system of partial differential equations describing the mechanical behavior. This approach promises various advantages: The unstructured grid allows for a good description of any geometry. Due to the possibility to divide the geometry into several subregions, the calculation can be carried out efficiently by a parallelization. The time-domain description will allow for the inclusion of non-linear properties in the future.

In an inverse design approach, the material parameters are determined on the basis of the electrical impedance of the respective piezoceramic by optimization with our software tool [1]. In order to be able to consider a freely selectable electrode structure, a three-dimensional structure without assumption of any symmetries is regarded in this work.

Here, the openCFS software [2] will be used to validate the results with respect to linear material dependencies of the electrical and mechanical properties and the required compute times. In order to compare the different methods, only a linear behavior on the electrical and mechanical quantity is considered.

Physical description of piezoceramics

The relationship between the mechanical (stress $\boldsymbol{T}$ and strain $\boldsymbol{S}$) and electrical (electric field strain $\boldsymbol{E}$ and flux density $\boldsymbol{D}$) components can be described by using the following linear system of equations in Voigt notation [3]:

$$\begin{aligned} \boldsymbol{T} &= \boldsymbol{c}^{\mathrm{E}}\boldsymbol{S} - \boldsymbol{e}^{\mathrm{t}}\boldsymbol{E} \\ \boldsymbol{D} &= \boldsymbol{e}\boldsymbol{S} + \boldsymbol{\varepsilon}^{\mathrm{S}}\boldsymbol{E} \end{aligned} . \tag{1}$$

The elastic stiffness matrix $\boldsymbol{c}^{\mathrm{E}}$, the piezoelectric constant $\boldsymbol{e}$ and the permittivity matrix $\boldsymbol{\varepsilon}^{\mathrm{S}}$ are required for the description. In this work the material parameter for PIC255 manufactured by PI Ceramic are used [4]. For general formulation, each node is given a set of material parameters.

The plane wave in the piezoceramic can be calculated and described with [5]

$$\begin{aligned} \rho_0 \frac{\partial^2 u_1}{\partial t^2} &= \frac{\partial T_1}{\partial x_1} + \frac{\partial T_6}{\partial x_2} + \frac{\partial T_5}{\partial x_3} \\ \rho_0 \frac{\partial^2 u_2}{\partial t^2} &= \frac{\partial T_6}{\partial x_1} + \frac{\partial T_2}{\partial x_2} + \frac{\partial T_4}{\partial x_3} \\ \rho_0 \frac{\partial^2 u_3}{\partial t^2} &= \frac{\partial T_5}{\partial x_1} + \frac{\partial T_4}{\partial x_2} + \frac{\partial T_3}{\partial x_3} \end{aligned} \tag{2}$$

with the mechanical stress

$$\boldsymbol{T} = \begin{bmatrix} c_{11}^{\mathrm{E}} \frac{\partial u_1}{\partial x_1} + c_{12}^{\mathrm{E}} \frac{\partial u_2}{\partial x_2} + c_{13}^{\mathrm{E}} \frac{\partial u_3}{\partial x_3} + e_{31} \frac{\partial \phi}{\partial x_3} \\ c_{12}^{\mathrm{E}} \frac{\partial u_1}{\partial x_1} + c_{22}^{\mathrm{E}} \frac{\partial u_2}{\partial x_2} + c_{23}^{\mathrm{E}} \frac{\partial u_3}{\partial x_3} + e_{32} \frac{\partial \phi}{\partial x_3} \\ c_{13}^{\mathrm{E}} \frac{\partial u_1}{\partial x_1} + c_{23}^{\mathrm{E}} \frac{\partial u_2}{\partial x_2} + c_{33}^{\mathrm{E}} \frac{\partial u_3}{\partial x_3} + e_{33} \frac{\partial \phi}{\partial x_3} \\ c_{44}^{\mathrm{E}} \left(\frac{\partial u_2}{\partial x_3} + \frac{\partial u_3}{\partial x_2} \right) + e_{15} \frac{\partial \phi}{\partial x_2} \\ c_{55}^{\mathrm{E}} \left(\frac{\partial u_1}{\partial x_3} + \frac{\partial u_3}{\partial x_1} \right) + e_{15} \frac{\partial \phi}{\partial x_1} \\ c_{66}^{\mathrm{E}} \left(\frac{\partial u_1}{\partial x_2} + \frac{\partial u_2}{\partial x_1} \right) \end{bmatrix} . \tag{3}$$

With Eq. (2) and Eq. (3), we obtain a system of equations that depend only on the mechanical displacement $\boldsymbol{u}$. With the special feature that terms consist of either double spatial or double temporal

DOI 10.5162/Ultrasonic2025/A18-a1

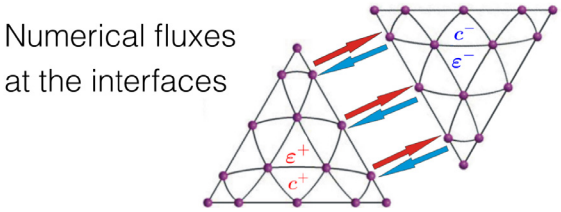

Fig. 1: Concept of the DG method with the numerical fluxes [7] (modified).

derivative terms. For the following numerical description, the sound velocity is introduced as the first time derivative of the mechanical displacement. This results in equations with first-order derivatives in space and time, which is necessary for the DG method.

Model

As an example, a piezoceramic cylinder ($r = 5\,\mathrm{mm}$, $h = 1\,\mathrm{mm}$) with full-surface electrodes is considered. For the simulations it is assumed that the piezoceramic can vibrate freely and does not experience any external forces. Therefore the following boundary condition is obtained:

$$\boldsymbol{N}^{\mathrm{t}}\boldsymbol{T} = 0, \tag{4}$$

where $\boldsymbol{N}^{\mathrm{t}}$ is the normal matrix of the respective boundary surface in Voigt notation.

Numerical scheme

This section provides an overview of the discontinuous Galerkin time domain method. The two main foundations are the DG operators and time stepping.

The DG method is related to two well-known methods: the Finite Element Method (FEM) and Finite Volume Method (FVM). The main difference is the range in which the shape functions extend. As in the FEM method, the computational domain is divided into triangles or tetrahedra. The shape functions of the DG method only apply locally in the computational domain. This allows local matrices to be set up, which have advantages in terms of individual calculation steps and parallelization [6]. The discontinuities between the neighboring volume elements can be corrected by the exchange of information with the so-called numerical fluxes f^*. This concept is illustrated in Fig. 1. The numerical flux is typically a function of internal and external values of the same coordinates. Where external describes the neighboring element or an external boundary condition and internal identifies the element in which the calculation takes place. Many different approaches for the numerical flux are presented in the literature [8]. Two fluxes are used in the following section. The central flux

$$f_{\mathrm{C}}^*(u) = \frac{f_-(u) + f_+(u)}{2} \tag{5}$$

can be interpreted mathematically as the mean value, this calculates the mean value of the two values present at the respective boundary node. To obtain a monotone solution, the central flux is extended to the Lax-Friedrichs flux as follows

$$f_{\mathrm{L}}^*(u) = \frac{f_-(u) + f_+(u)}{2} + \frac{C_{\mathrm{w}}}{2} n\,(u_- - u_+)\,, \tag{6}$$

where C_{w} describes the maximum speed of sound of the material.

To solve the piezoelectric equations, a first-order system is required in the DG method. To do this, the Eq. (2) and Eq. (3) are rewritten into the conservation form. The computational domain Ω is divided into K non-overlapping tetrahedra, where k indicates the k-th element.

$$\Omega = \bigcup_{i=1}^{K} D^k. \tag{7}$$

Eq. (8) describe the acoustics wave in the piezoceramic, which is approximated using the vectors u_i^k, which describe the DG approximation in the respective element k. In each element k, the function $u(x,t)$ is approximated as $u^k(x,t)$ using

$$u^k(x,t) = \sum_{i=1}^{N_p} u^k(x_i^k, t) l_i^k(x) \;\forall k \in K \tag{8}$$

with Lagrange polynomials $l_i^k(x)$ in the k-th node. In order to be able to apply the operators to every volume element k in general, a reference element is defined and an assignment is created. In this reference element, an unstructured grid with N_p

$$N_p = \frac{(N+1)\,(N+2)}{N} \tag{9}$$

nodes is generated, where N indicates the polynomial order of the basis functions.

In the DG method, the functions are implemented using operators. The mass matrix $\boldsymbol{M}$, the stiffness matrix $\boldsymbol{A}$ and the derivative operators $\boldsymbol{D_x}$ and $\boldsymbol{D_z}$ are required. The spatial derivatives can be approximated with the differentiation matrix:

$$\frac{\partial}{\partial x} \approx \boldsymbol{D_x} \tag{10}$$

In the DG method, the equation for the mechanical

DOI 10.5162/Ultrasonic2025/A18-a1

stress T_1 can be described for each node k using

$$\begin{aligned} T_1^k &= c_{11}^{\mathrm{E},k} D_{x_1}^k u_1^k + c_{12}^{\mathrm{E},k} D_{x_2}^k u_2^k \\ &+ c_{13}^{\mathrm{E},k} D_{x_3}^k u_3^k + e_{31}^k D_{x_3}^k \phi^k \\ &- M_k^{-1} c_{11}^{\mathrm{E},k} \oint_{\partial D^k} n_{x_1}^k \left(u_1^k - u_{1\mathrm{C}}^{k*}\right) l^k \mathrm{d}x \\ &- M_k^{-1} c_{12}^{\mathrm{E},k} \oint_{\partial D^k} n_{x_2}^k \left(u_2^k - u_{2\mathrm{C}}^{k*}\right) l^k \mathrm{d}x \\ &- M_k^{-1} c_{13}^{\mathrm{E},k} \oint_{\partial D^k} n_{x_3}^k \left(u_3^k - u_{3\mathrm{C}}^{k*}\right) l^k \mathrm{d}x. \end{aligned} \tag{11}$$

Here D^k and $c^{\mathrm{E},k}$ represent the respective location-dependent values for node k. The central flux f_{C}^* is used for the mechanical stress. The other components of the mechanical stress $\boldsymbol{T}$ are described in the same way. The time derivative of the sound velocity $\boldsymbol{v}$ and the displacement $\boldsymbol{u}$ is described using

$$\begin{aligned} \frac{\partial v_1^k}{\partial t} &= \frac{1}{\rho^k} D_{x_1}^k T_1^k + \frac{1}{\rho^k} D_{x_3}^k T_5^k \\ &- M_k^{-1} \frac{1}{\rho^k} \oint_{\partial D^k} n_{x_1}^k \left(T_1^k - T_{1\mathrm{L}}^{k*}\right) l^k \mathrm{d}x \\ &- M_k^{-1} \frac{1}{\rho^k} \oint_{\partial D^k} n_{x_2}^k \left(T_6^k - T_{6\mathrm{L}}^{k*}\right) l^k \mathrm{d}x \\ &- M_k^{-1} \frac{1}{\rho^k} \oint_{\partial D^k} n_{x_3}^k \left(T_5^k - T_{5\mathrm{L}}^{k*}\right) l^k \mathrm{d}x \\ \frac{\partial u_1^k}{\partial t} &= v_1^k. \end{aligned} \tag{12}$$

Here the Lax-Friedrichs flux is used.

Parallelization

To ensure efficient use of the simulation tool, emphasis is placed on computing time optimization and parallelization. The Message Passing Interface (MPI) library makes it possible to communicate between the processes and exchange data.

To optimally partition the entire computational domain into several smaller, non-overlapping subdomains, the Parallel Graph Partitioning and Fill-reducing Matrix Ordering library (ParMetis) is employed.

By combining these two libraries and the advantages of the DG method, the computing time can be reduced and the available computing resources can be fully exploited.

Time domain integration

The time step for the respective integration method is decisive for the numerical stability. In this case, the low storage explicit Runge Kutta (LSERK) [8] of the fifth order is used. To estimate a time step, the initial wave velocity v_{init}, the radius of the inner sphere of the volume element r_D and the distance between two parallelization elements Δr_i are required [9]

$$\Delta t \leq \frac{2}{3} \min\left(\Delta r_i\right) \min_{\Omega} \left(\frac{r_D}{|v_{\mathrm{init}}|}\right). \tag{13}$$

The interaction between the time step and the flux has a massive influence on the numerical stability. The stability can be positively influenced by the choice of the Lax-Friedrichs flux. Simulations involving higher-order shape functions typically exhibit greater instability.

Validation

In order to validate the results of the simulations, Hook's law is considered here. This represents the relationship between the mechanical stress $\boldsymbol{T}$ and the displacement $\boldsymbol{u}$.

The following distribution of the mechanical stress

$$T_3 = 10^9 \cdot e^{\left(-\frac{\left(z - 5\times10^{-4}\,\mathrm{m}^{-1}\right)^2}{10^{-8}}\right)} \cdot \sin\left(2 \times 10^3\,\mathrm{m}^{-1} \cdot \pi \cdot z\right) \tag{14}$$

is specified as the initial condition of the simulation. It is to be expected that the imprinted wave propagates within the model and is reflected at the edges of the computational domain. Consideration of the boundary conditions is essential here. The equation can be incorporated directly on the two cover surfaces. For the cladding of the piezoceramic, some modifications must first be made. The following equations

$$\begin{aligned} n_x T_1 + n_y T_6 + n_z T_5 &= 0 \\ n_x T_6 + n_y T_2 + n_z T_4 &= 0 \\ n_x T_5 + n_y T_4 + n_z T_1 &= 0 \end{aligned} \tag{15}$$

form the boundary conditions for the mechanical stress $\boldsymbol{T}$ in 3D. For the implementation, the mechanical stress is rotated so that the normal vector only has one nonzero component. The boundary condition is then imprinted and the mechanical stress is rotated back to its original state. This method proved to be robust.

During the tests, it became clear, that besides a well chosen time step, the underlying computational grid also has an huge influence on the simulation results. A high-quality grid in which the elements have uniform shapes and volumes, is necessary for a stable simulation.

Results

The work has shown that the advantages of the DG method can be used for the numerical simulation of the mechanical behavior. A stable simulation is possible by selecting a polynomial order and a suitable computational grid. Additionally, it is shown that the exact numerical consideration of the boundary conditions is important for numerical stability.

DOI 10.5162/Ultrasonic2025/A18-a1

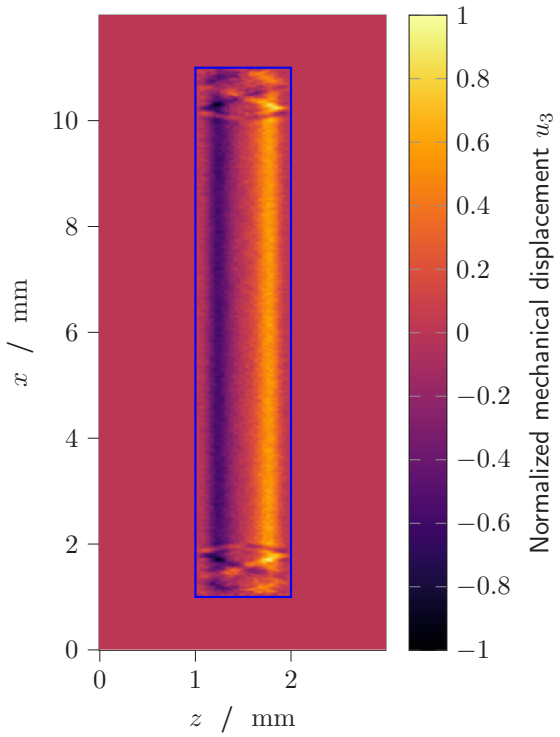

Fig. 2: Normalized simulation results in the x-z plane using the initial condition Eq. (14).

Fig. 2 shows the field of mechanical displacement in the x-z plane, i.e. a cross-section through the piezoceramic. The inner area of the blue rectangle indicates the piezoceramic, the outer area is used to imprint the boundary conditions. Reflections on the edges of the piezoceramic can be clearly recognised. In particular, the superimposition of the reflections on the cladding and the cover surfaces are well depicted. This is necessary for future calculations of the resonance frequencies, which is necessary for estimating the material properties [1].

It has been shown that stability decreases in simulations with a large number of time steps due to numerical instabilities. The geometry of the computational domain was varied in secondary work. In conclusion, it can be said that with the right choice of boundary conditions, the software tool can be used universally.

The work presented here shows the simulation of wave equation as a basis for the description of the mechanical waves in a piezoceramic. To summarize, the extension of the DG code provides a solid basis for further development in this field.

In future work, the coupling of the electrical quantity such as the electrical potential will be investigated.

Acknowledgements

The authors would like to thank the German Research Foundation (DFG) for funding the project 444955436 (NEPTUN). The authors would also like to express their gratitude to the Paderborn Center for Parallel Computing (PC^2) for access to the Noctua 2 cluster.

References

[1] N. Feldmann et al. In: *tm - Technisches Messen* 87.s1 (2020), s50–s55. DOI: doi:10.1515/teme-2020-0012. URL: https://doi.org/10.1515/teme-2020-0012.

[2] openCFS development team. *openCFS – open-source simulation tool for coupled field problems*. Accessed: 2025-06-16. 2025. URL: https://gitlab.com/openCFS/cfs.

[3] W. Voigt. *Lehrbuch der Kristallphysik (mit Ausschluss der Kristalloptik)*. Vieweg+Teubner Verlag, 1928. ISBN: 978-3-663-15316-0.

[4] C. Unverzagt. "Sensitivitätssteigerung durch Elektrodenmodifikation für die Materialparameterbestimmung von Piezokeramiken". PhD thesis. PhD thesis. Paderborn University, 2018. DOI: https://doi.org/10.17619/UNIPB/1-311.

[5] J. D. N. Cheeke. *Fundamentals and Applications of Ultrasonic Waves*. CRC Series in Pure and Applied Physics. Boca Raton, FL: CRC Press, 2002. ISBN: 0-8493-0130-0.

[6] Y. Grynko and J. Förstner. "Simulation of Second Harmonic Generation from Photonic Nanostructures Using the Discontinuous Galerkin Time Domain Method". In: *Recent Trends in Computational Photonics*. Springer International Publishing, 2017.

[7] Y. Grynko. *Numerical Simulations with the Discontinuous Galerkin Time Domain Method*. Lecture Slides, Paderborn University. 2021.

[8] T. W. Jan S. Hesthaven. *Nodal Discontinuous Galerkin Methods*. Springer New York, NY, 2007. DOI: https://doi.org/10.1007/978-0-387-72067-8.

[9] E. Brodal, J. S. Hesthaven, and F. Melandsø. "Numerical modeling of double-layered piezoelectric transducer systems using a high-order discontinuous Galerkin method". In: *Computers & Structures* (). DOI: https://doi.org/10.1016/j.compstruc.2008.02.006.